

Impact of different layers on performance of OLED

Shubham Negi¹ · Poornima Mittal² · Brijesh Kumar³

Received: 23 December 2017 / Accepted: 20 April 2018 / Published online: 4 May 2018

© Springer-Verlag GmbH Germany, part of Springer Nature 2018

Abstract

This paper explores how different layers in an organic light emitting diode (OLED) impacts its performance. Here, different layers of OLED similar to hole/electron injection layer, transport layer, and block layers are analyzed. Four experimental devices are taken into consideration and their results are compared to one over another to analyze the impact of every layer. Inside depth analysis is also performed on the device to inspect what really is happening innermost of the OLED. It is noticed that hole and electron block layer are instrumental in improving the device luminescence performance and efficiency. There is an improvement of 16, 37 and 38% in the luminescence of the device when hole block layers and electron block layers are added. Internal device analysis reveals that increase in charge carrier concentration and carrier confinement are the reason for this improvement.

1 Introduction

Organic electronics, in the past decades, has been the choice of researchers to complement the conventional silicon-based technology. These devices are being preferred because of the fact that they are lightweight (Chou et al. 2017), thin, flexible, easy to fabricate with a *low-cost* (Chou et al. 2017; Kumar et al. 2014; Fu et al. 2016) involved in manufacturing. Because of this intense research, recent times have seen different applications based on organic transistors, like memory and digital circuits, which have shown good performance. Because of this improvement other applications like OLED, RFID etc. are also emerging and improving.

Organic light emitting diodes (OLEDs), at present time, are at the apogee of display technology research. The main

reasons for this are their flexible nature (Chou et al. 2017), low temperature (Fu et al. 2016) and low-cost fabrication (Yu et al. 2015, Manna et al. 2015) and ability to be fabricated on a large surface (Dodabalapur 1997). This is complemented by good performance characteristics such as a huge gamut of colors it can emit, low power requirement, wide viewing angle (Kumar et al. 2014; Yu et al. 2015), etc. This is one of the main reasons companies like Apple and Samsung are exploiting these devices in a display application. However, its applications are not just limited to displays. These devices also show good luminescence properties emitting a uniform color of light (Dodabalapur 1997). These properties can be utilized for other applications such as sensors (Manna et al. 2015) OLED bulbs, visual light communication (VLC) (Ohmori et al. 2004; Haigh et al. 2013) and other portable applications as well.

Currently, OLED is being used by companies like Apple and LG for the display application. Still, a number of researchers are trying to further enhance its performance. Different strategies are being followed to improve the performance of OLED. Some of them are static in the sense that these will work in a specific way like a material design (Malliaras et al. 2001; Chan et al. 2001; Wen et al. 2005), which will work with a specific set of materials only. Others are dynamic like the use of block layers in architecture (Yang et al. 2006) and change of electrode material (Wu et al. 2007) in which, depending on the architecture different materials can be used. Herein, the work carried out is related to the latter aspect wherein different materials can be used in OLED architecture to enhance its

✉ Poornima Mittal
poornima2822@ieee.org

Shubham Negi
shubham.negi.1992@ieee.org

Brijesh Kumar
bkece@mmmut.ac.in

¹ Department of Electronics and Communication Engineering, Graphic Era University, Dehradun 248002, India

² Department of Electronics and Communication Engineering, Delhi Technological University, Delhi 110042, India

³ Department of Electronics and Communication Engineering, M. M. M. University of Technology, Gorakhpur, UP, India

performance. Various analyses of different layers in a multilayered OLED architecture are provided wherein; these analyses cover how these different layers help in enhancing OLED performance.

This article is divided into five parts with the inclusion of this introductory part. In Sect. 2, basic architecture of OLED along with different layers that can be used in its architecture is explained. This is followed by an analysis of different OLEDs and their results in Sect. 3. Thereafter, in Sect. 4, results of the analysis are discussed and more internal device analyses to support the results are given. Thereafter paper is concluded by remarks given in Sect. 5.

2 OLED architecture

The light generation in both, conventional LED (Wakui et al. 2011) and OLED, is because of recombination of electrons and holes. Still, there are a lot of differences in them ranging from architecture to carrier transport, and processes governing recombination rate. In an organic semiconductor (OSC) mobility is low, and doping is not possible (Kumar et al. 2014; Dodabalapur 1997). Further, minority carriers are not present as their mobility is even lower. Moreover, the recombination is not governed by recombination rate but by the probability of charge carriers finding themselves according to Langevin theory. Hence the basic architecture of OLED given by Tang and Slyke (Kumar et al. 2014) consisted of two layers of OSC, one being *p*-type and the other being *n*-type as shown in Fig. 1.

The basic OLED structure consists of an anode and a cathode, which are surrounding two OSCs, one of which is *p*-type responsible for hole transport (HTL) and the other is *n*-type responsible for electron transport (ETL) (Dodabalapur 1997). When a proper biasing is given to this circuit holes enter from the anode into HTL and electrons from the cathode into ETL. Ideally, as shown in Fig. 1, these charge

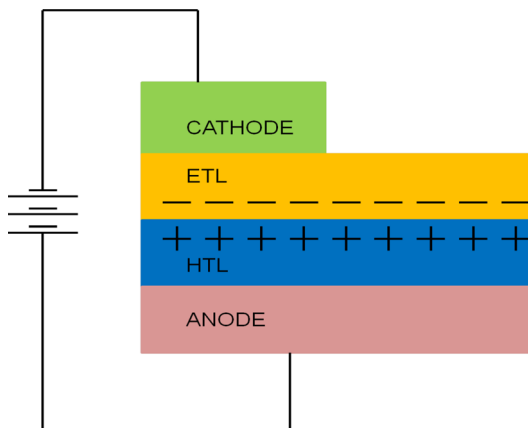


Fig. 1 The basic architecture of OLED

carriers should meet at the interface of HTL and ETL and recombination should take place.

However, the organic materials developed so far have a very low electron mobility compared to hole mobility. This causes the recombination to take place not at the interface but near the cathode. Moreover, holes having a higher mobility often reach the cathode and carrier quenching takes place (Park et al. 2007, 2009; Park 2010). This led to the poor performance of OLED in the beginning.

Researchers have suggested different methods to counter this problem. Use of different layers to balance charge injection (Park et al. 2007, 2009; Park 2010) is one of them. These layers are used in conjunction with each other to form a multilayered architecture. One by one a brief discussion about each of these layers is given. Figure 2 shows the structure of multilayered OLED. It shows each and every layer along with the functions that these layers can perform.

2.1 Emission layer (EML)

It is the layer responsible for the emission of light in an OLED. Preferably all the recombination in an OLED should take place here. It may be a single layer or a group of layers like, in Fig. 2, QAD along with Alq₃ (Karatsu 2015; Li et al. 2006; van Veldhoven et al. 2001) is acting as an emission layer. EML is responsible for emissive properties of an OLED like color and luminescence.

2.2 Hole and electron transport layers (HTL/ETL)

The mobility of electrons and holes are different for different OSCs. In an OLED a balance charge injection is required and for this purpose, it is required that electron and hole mobility should be as close as possible. The purpose of the transport layer is to ease the flow of charge

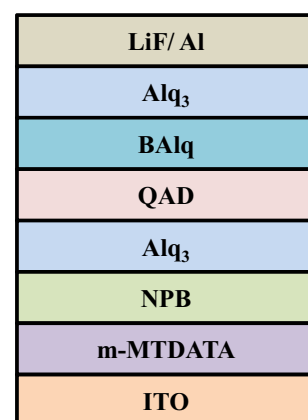


Fig. 2 Structure of multilayered layer OLED showing different layers used

carriers to emission layer (Yu et al. 2015). They should preferably have a high mobility and their highest occupied molecular orbital (Park et al. 2007) (HOMO) level (for holes) and lowest unoccupied molecular orbital (Park 2010) (LUMO) level (for electrons) should be matched with respective levels of EML layer.

2.3 Hole and electron injection layers (HIL/EIL)

HOMO and LUMO level of OSC plays an important role in charge carrier injection. If these levels are matched with the work-function of adjacent electrode then charge injection in the OLED will improve which will result in higher charge carriers and ultimately recombination. HIL (Park et al. 2007) and EIL (Park et al. 2009) layers are used for this purpose. These layers are selected depending on their orbital levels, i.e. HOMO for HIL and LUMO for EIL and matching of these levels to the work function of respective electrodes. The closer these two levels are, the better is the charge injection. These layers help more and more charge carriers to reach respective transport layers as the energy barrier is reduced between transport layers and electrode work-function. This is shown in energy band diagram given in Fig. 3. Thus better charge injection improves the recombination rate.

2.4 Hole and electron block layer (HBL/EBL)

Charge carrier quenching is an important issue in which the higher mobile charge carrier reaches the opposite electrode and gets exhausted there. These charge carriers do not help in recombination and thus reduces the device efficiency. Hence, there is a need to prevent these charge carriers from reaching opposite electrodes. Block layers (Yang et al. 2006) fulfil this purpose. These layers block the respective charge carriers. This task is again achieved by modelling the energy levels of these layers. Like for blocking the holes, hole block layers (HBL) are chosen such that there is

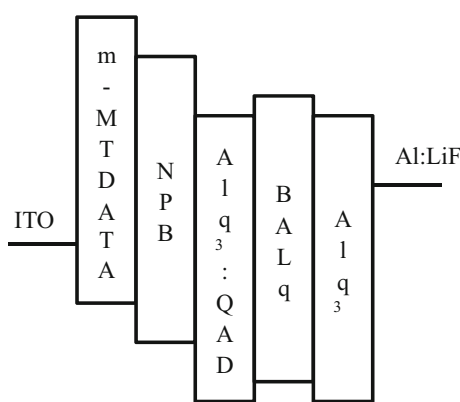


Fig. 3 Energy band diagram of multilayer OLED

a high energy gap between HOMO levels of EML and HBL. This high energy gap as shown in Fig. 3 between QAD (EML) and BAQ (HBL) layer prevents holes from crossing EML. Thus charge carrier concentration in EML increases which improve recombination probability.

3 Experimental setup and fabrication procedure

This article analyses the impact on the performance of OLED when different layers are added to multilayered architecture. The tool used for this purpose is Atlas by Silvaco. It uses the *Poole and Frenkel* mobility model (ATLAS 2014) for analysis of characteristics of organic devices. This model is given by the following equation:

$$\mu(E) = \mu_0 \exp \left[-\frac{\Delta}{KT} + \left(\frac{\beta}{KT} - \gamma \right) \sqrt{E} \right], \quad (1)$$

where $\mu(E)$ is the field dependent mobility, E is electric field, μ_0 is null field mobility, Δ is activation energy, β is Hole Poole Frenkel Factor $= q\sqrt{q/\pi\epsilon\epsilon_0}$ and γ is the fitting parameter.

On the other hand, *Langevin Recombination Model* (ATLAS 2014) is followed for the analysis of carrier recombination and excitons formation in the OLED. The recombination rate in this model also known as Langevin Recombination rate and it is given by the following equation:

$$R_L(n, p) = r_l(x, y, t) (np - n_i^2), \quad (2)$$

where r_l is Langevin recombination rate coefficient, n_i is intrinsic concentration, n (/p) is electron (/hole) concentration and Langevin recombination rate coefficient is given by the following equation:

$$r_l(x, y, t) = \frac{q\mu(E)}{\epsilon_r \epsilon_0}, \quad (3)$$

where q is charge of electron, ϵ_r is relative permittivity of OSC and ϵ_0 is absolute permittivity.

The analysis process starts with taking a fabricated device and simulating it through Atlas. This device will be the reference device, Device A. In this work, a multilayered OLED (Yang et al. 2006) is taken as a basic reference device. This device was fabricated by Yang et al. (2006). The structure of this device is shown in Fig. 4a which clearly shows the position of each layer used in the device architecture. The dimensions of each layer used are also marked in the Fig. 4a itself and are also given in Table 1 (Yang et al. 2006). This is followed by a brief description of different processes through which each of these layers can be deposited so that the device can be fabricated.

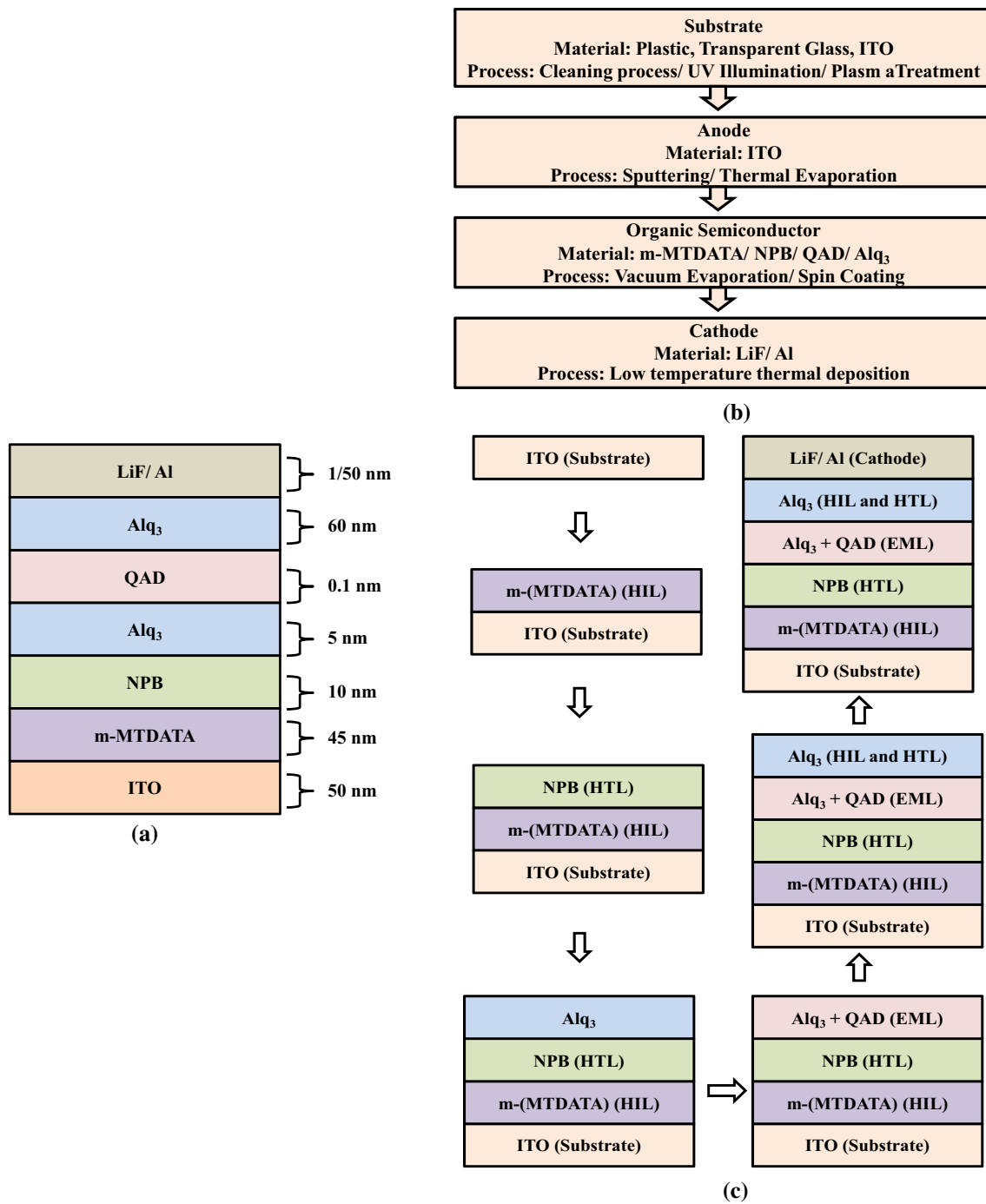


Fig. 4 **a** Structure of multilayered OLED, Device A, **b** basic flow diagram for fabrication of OLED and **c** specific and complete fabrication flow for Device A

Therefore, along with this, a basic flow diagram for fabrication of OLED is given in Fig. 4b. This is followed by the specific fabrication flow diagram for composing Device A in Fig. 4c.

The fabrication process of the OLED device starts with indium tin oxide (ITO) glass as a substrate. Normally the ITO glass is cleaned by scrubbing and sonication processes

and thereafter rinsed in DI water followed by drying in an oven (Yang et al. 2006). Sometimes, ITO can be subjected to other cleaning processes such as cleaning it in ethanol and acetone and followed by UV illumination (Li et al. 2012) or plasma treatment (Samal et al. 2009) depending on the need and availability of materials. Further, if ITO is not being used as a substrate, then it can be deposited over

Table 1 Dimension of multi-layered OLED

S. no.	Layer name	Device A (dimensions in nm)
1.	Al	50
2.	LiF	1
3.	Alq ₃	60
4.	QAD	0.1
5.	Alq ₃	5
6.	NPB	10
7.	m-MTDATA	45
8.	ITO	50

some other substrate such as glass by using sputtering process (Li et al. 2006). Thereafter, it can be followed by cleaning processes as given above and dried in an oven.

This is followed by deposition of different organic layers on the cleaned ITO/glass substrate by either by vacuum evaporation or by spin coating. The vacuum evaporation process is carried out at high pressure (10^{-6} – 10^{-7} Torr) (Yang et al. 2006; Samal et al. 2009) and temperature ranging to 60–80 °C. For spin coating process a suitable solvent is taken in which the material whose layer has to be deposited can be dissolved. Thereafter, it is spin coated on the substrate and dried to evaporate the solvent (Li et al. 2006). The thickness of each layer is closely monitored by different methods for example oscillating quartz thickness monitor (Yang et al. 2006). The organic layers used in this reference device are m-MTDATA (4,4',4''-Tris[(3-methylphenyl)phenylamino]triphenylamine) as hole injection layer, NPB (*N,N'*-Di(1-naphthyl)-*N,N'*-diphenyl-(1,1'-biphenyl)-4,4'-diamine) as hole transportation layer, Alq₃ (Tris(8-hydroxyquinolato)aluminum) as electron injection and transportation layer. QAD has been used as emission layer in combination with Alq₃.

Finally, the cathode, a bilayer of LiF and Al are thermally deposited (Yang et al. 2006; Li et al. 2012). Normally, the deposition takes place at a low temperature, because high temperature processes can damage the organic materials. Hence, deposition is carried under high pressure and a low temperature (60–80 °C).

This is followed by the device analyses and the results of the fabricated device and the experimental device are compared. These results are given in Fig. 5. This device is taken as Device A. It can be seen from Fig. 5a, b that there is a close match between fabricated and the experimental results. The comparative results of device analysis are given in Table 2.

This reference device, Device A consists of charge injection layer, transport layers, and the emission layer. When compared to the basic device consisting of just two

layers of OSC this device performance is far exceeding. Now, after these layers, hole block layers (HBL) are incorporated in multilayer device architecture. First, a single hole block layer BAlq (Bis(8-hydroxy-2-methylquinoline)-(4-phenylphenoxy)aluminum) is added to the device. This layer is placed next to the emission layer. This device is Device B. Its dimensions are given in Table 3. The analyses results of the Device B are shown in Fig. 6. It is clear from Fig. 6 that luminescence of Device B is better than that for Device A; however, its current density is very low. The reason for this low current density is that holes are being blocked by HBL and hence these blocked charge carriers are not able to contribute to any current.

After this, a double hole block layer device, Device C, is analyzed. This device consists of two HBLs, BAlq and BPhen (4,7-Diphenyl-1,10-phenanthroline), adjacent to EML layer. Device dimensions of this device are given in Table 3 as well. It is to be noted here is that even though a new layer is added, still the overall device dimension is same as Device B because, in Device C, the thickness of two HBLs has been halved (8 nm) as compared to that in Device B (16 nm). Its structure is shown in Fig. 7.

Analysis results of this device are shown in Fig. 8. The results of the analysis show that there is a clear improvement in the luminescence of Device C, which shows the maximum luminescence. The current densities for this device are still lower than Device A and the reason for this being that HBLs are blocking the holes, but at the same time, it is higher than Device B.

Now the reason for this improvement in current density for Device C over Device B may be attributed to the increase in charge carrier injection because these two HBL not only blocks the holes but at the same time increases the electron injection as well. This is because the LUMO levels of these layers are in midst of EML layer and EIL (Alq₃) layer. Finally, as the hole block layers are quite efficient in improving the performance of OLED, one more device is analyzed. In this device hole injection layer (HIL) m-MTDATA in Device C was changed with Ir(ppz₃) layer. The reason for this being the LUMO level of this layer was higher than m-MTDATA, so it will help in restricting the movement of electrons and HOMO level is similar to m-MTDATA. Device dimensions of this device are given in Table 3.

Analysis results for Device D are shown in Fig. 9a, b. Figure 9a shows the results for current density versus anode voltage and Fig. 9b shows the results for luminescence versus anode voltage. Further, the comparative results of all the analyzed devices (Device A–D) are given in Fig. 10a, b. The former of the two figures show the results for current density and the latter for luminescence for all the analyzed devices. It can be noticed from Fig. 9

Fig. 5 Comparison of result for fabricated and experimentally analyzed device. **a** Current density v/s anode voltage, and **b** luminescence v/s anode voltage

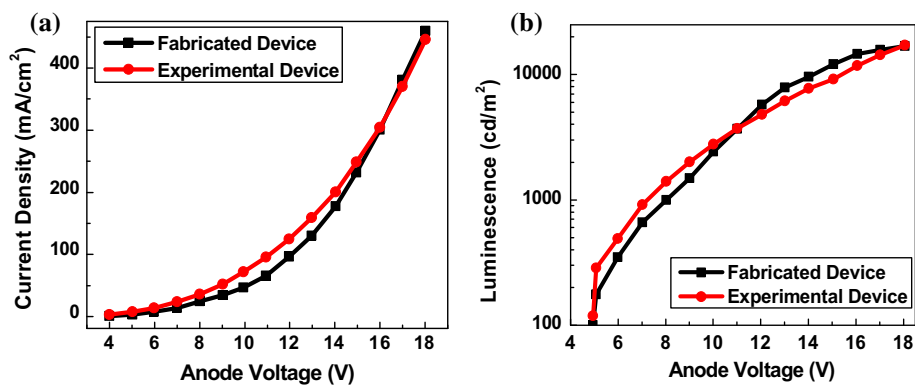


Table 2 Comparative data for fabricated and experimental device

S. no.	Parameter name	Fabricated device	Experimental device	Deviation (%)
1.	Current density (mA/cm ²)	459.86	445.79	3.05
2.	Luminescence (cd/m ²)	16,916	17,190	1.6

Table 3 Dimensions of Device B and Device C, single hole block layer OLED

S. no.	Name of the layer	Dimension (nm)		
		Device B	Device C	Device D
1.	ITO	50	50	50
2.	Ir(ppz ₃)	—	—	45
2.	m-MTADATA	45	45	—
3.	NPB	10	10	10
4.	Alq ₃	5	5	5
5.	QAD	0.1	0.1	0.1
6.	Alq ₃	10	10	10
7.	BPhen	—	8	8
8.	BAlq	16	8	8
9.	Alq ₃	44	44	44
10.	LiF	1	1	1
11.	Al	50	50	50

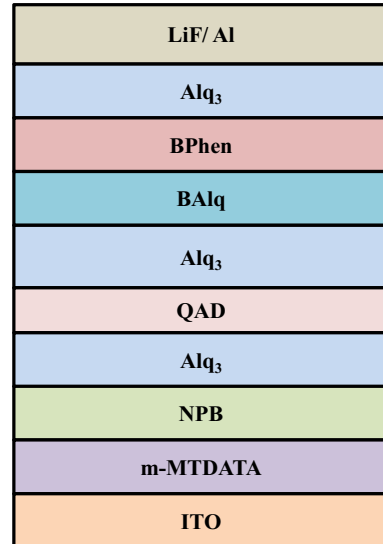


Fig. 7 Structure of double hole block layer OLED

Fig. 6 Analysis results for Device B. **a** Current density v/s anode voltage and **b** luminescence v/s anode voltage

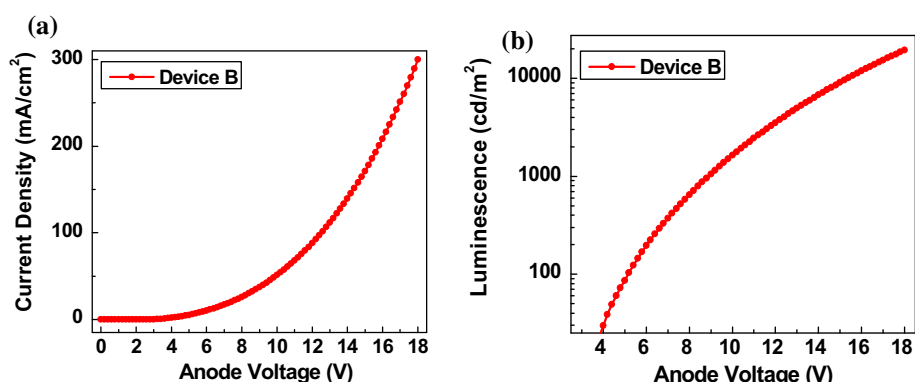


Fig. 8 Analysis results for Device C, **a** current density v/s anode voltage and **b** luminescence v/s anode voltage

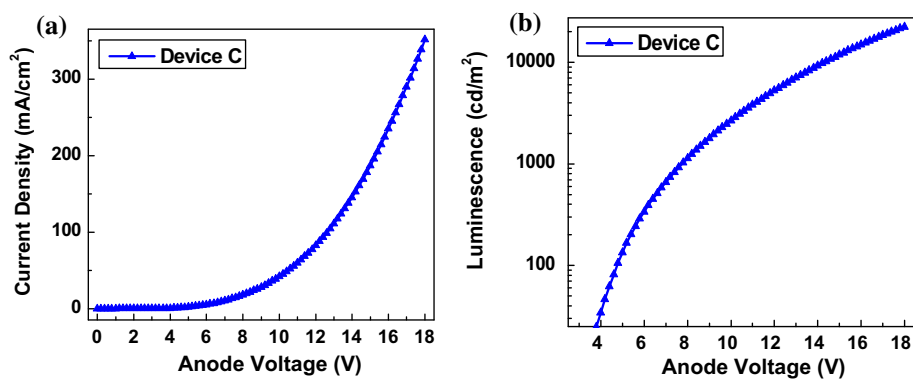


Fig. 9 **a** Analysis results for Device D current density v/s anode voltage and **b** luminescence v/s anode voltage

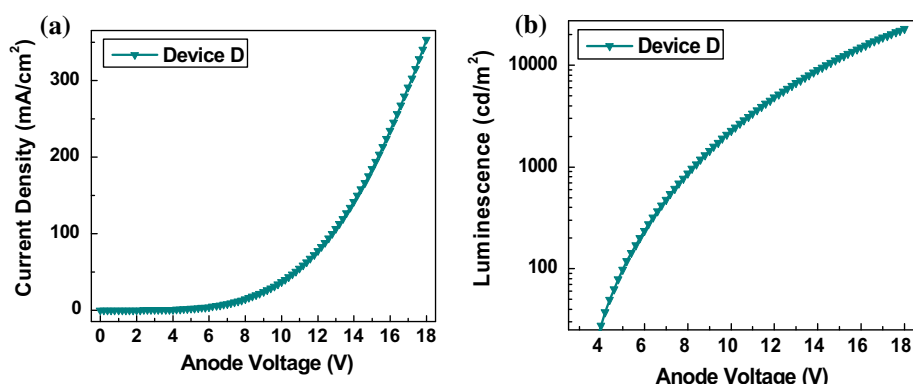
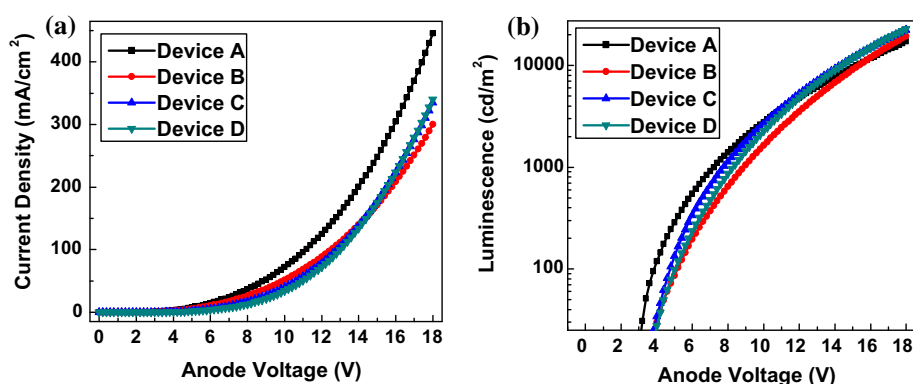


Fig. 10 Combined result for all the analysed devices (A–D). **a** Current density v/s anode voltage comparison, and **b** Luminescence v/s anode voltage comparison



that there is only a slight improvement in luminescence of OLED as compared to previous devices. The current density of this device is also similar to Device C. So there is not much improvement in device performance. In next section, reasons for these results are discussed and are supported by internal device analysis. A comparative analysis of data is tabulated in Table 4.

Table 4 Comparison of analysis of Device A–D

Property	Device A	Device B	Device C	Device D
Current density (mA/cm ²)	445.79	299.77	354.01	356.42
Luminescence (cd/m ²)	17,190	19,444.4	23,722	23,750.69
Luminescence power efficiency (lm/W)	6.73	11.32	11.70	11.34

4 Results and discussions

In the previous section, it is seen that hole block layers and electron block layers can improve the performance of OLED. Four devices (Device A–D) were analyzed and their performances were compared to each other. It was found out that double HBL device, Device C, had the best

performance and Device D with a change in EBL had a luminescence performance comparable to Device C. The results of this analysis are summed up in Table 4. Along with these results Table 4 also gives the luminescence power efficiency of these OLEDs which have been calculated with the help of following equation (Müllen and Scherf 2006).

$$\eta_P = \frac{L\pi}{JV}, \quad (4)$$

where L is luminance, J is the current density and whereas V is working voltage.

Table 4 shows that there is an improvement for luminescence of device along with luminescence power efficiency even though current density is reduced. This improvement in luminescence and decrement in current density is because of blocking layers. These block layers restrict the flow of charge carriers. As charge carriers movement is blocked thus current is reduced and at the same time, it increases the charge carrier concentration. This improves the probability of recombination and according to Langevin's theory, it will improve recombination rate. Theoretically, it was all good that charge carriers are blocked and thus recombination rate is improving. But to prove that it was really happening inside the device internal device analysis were performed using Atlas Silvaco tool and the result of analysis are shown in Fig. 11.

Figure 11 shows the electron and hole concentration for all four analyzed devices. It is clear from the figure that electron and hole concentration is highest in Device C and D and thereafter in Device B. All these three devices are having hole block layers. Further, it can be noticed that in Device C and D, there is better carrier confinement near emission layer as compared to other two devices, especially Device A. Hole concentration in Device C and D are confined to a much smaller region around the emission layer. Whereas, for Device A it is much wider. Further, the charge concentration for Device B, C and D is highest around 0.12 μm mark as compared to Device A. This is the

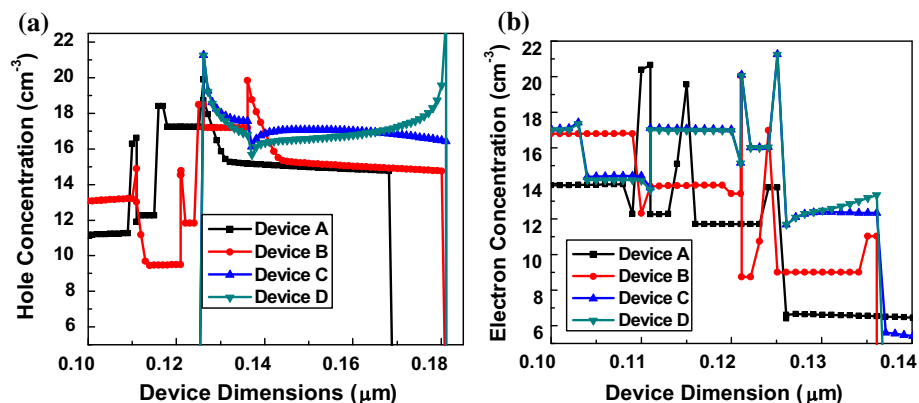
region of emission layer thus the higher charge concentration in this region helps improves the recombination rate and in the end luminescence properties of OLED.

5 Conclusion

In this paper, the impact of different layers on the performance of has been analyzed. It is known that the performance of multilayered OLED is better in compared to single and double layer OELD. This improvement in performance is due to the different layers included in its architecture. Four devices are compared in this paper, starting form multilayered device, Device A (consisting of HIL, EIL, and EML) and thereafter, hole block layer and electron block layers are added in Device B (single HBL), Device C (double HBL) and Device D (change in HIL, to EBL). When these devices are analyzed it was found out that compared to Device A, there is 16, 37 and 38% improvement in luminescence properties for Device B, C, and D respectively. Furthermore, the luminescence power efficiency for these devices turns out to be 6.73, 11.32, 11.70 and 11.34 (Device A–D) respectively.

Enhancement in charge carrier concentration of devices are HBL and EBL layers that are also the reasons for this improvement in performance. Internal device analysis are performed on each of these devices and it was seen from the results that indeed charge concentration is improved because of block layers and thus performance improvement is recorded. Further, in a device having double HBL (Device C and D), the carrier is much more confined to emission layer as compared to other devices. Therefore, luminescence is recorded highest in these devices. Thus it can be concluded that the block layers are instrumental in improving the performance of the device. Further if chosen wisely they can help in improving device performance without increasing the dimensions of the device.

Fig. 11 Internal device analysis of Device A–D. **a** Hole concentration and **b** electron concentration



References

ATLAS (2014) ATLAS User's Manual Device Simulation Software. Silvaco International Ltd, Santa Clara

Chan LH, Yeh HC, Chen CT (2001) Blue light-emitting devices based on molecular glass materials of tetraphenylsilane compounds. *Adv Mater* 13(21):1637–1641

Chou KY, Chao PCP, Chen CX, Wu CX, Huang SC (2017) Modeling and analysis of touch on flexible ultra-thin touch sensor panels for AMOLED displays employing finite element methods. *Microsyst Technol* 1(10):5211–5220

Dodabalapur A (1997) Organic light emitting diodes. *Solid State Commun* 102(2–3):259–267

Fu Y, Tsai CC, Tsai JL (2016) Characterizing mechanical behaviors of a flexible AMOLED during the debonding process. *Microsyst Technol* 22(10):2397–2406

Haigh PA, Ghassemlooy Z, Papakonstantinou I, Le Minh H (2013) 2.7 Mb/s with a 93-kHz white organic light emitting diode and real time ANN equalizer. *IEEE Photonics Technol Lett* 25(17):1687–1690

Karatsu T (2015) Materials for organic light emitting diode (OLED). Springer Ser Mater Sci 209:227–251

Kumar B, Kaushik BK, Negi YS (2014) Organic thin film transistors: structures, models, materials, fabrication, and applications: a review. *Polym Rev* 54(1):33–111

Li W, Jones RA, Allen SC, Heikenfeld JC, Steckl AJ (2006) Maximizing Alq₃/OLED internal and external efficiencies: charge balanced device structure and color conversion outcoupling lenses. *J Disp Technol* 2(2):143–152

Li F, Zhang Y, Wu C, Lin Z, Zhang B, Guo T (2012) Improving efficiency of organic light-emitting diodes fabricated utilizing AZO/Ag/AZO multilayer electrode. *Vacuum* 86(12):1895–1897

Malliaras GG, Shen Y, Dunlap DH, Murata H, Kafafi ZH (2001) Nondispersive electron transport in Alq₃. *Appl Phys Lett* 79(16):2582–2584

Manna E, Xiao T, Shinari J, Shinari R (2015) Organic photodetectors in analytical applications. *Electronics* 4(3):688–722

Müllen K, Scherf U (eds) (2006) Organic light emitting devices: synthesis, properties and applications. Wiley, New York

Ohmori Y, Kajii H, Kaneko M, Yoshino K, Ozaki M, Fujii A, Taneda T (2004) Realization of polymeric optical integrated devices utilizing organic light-emitting diodes and photodetectors fabricated on a polymeric waveguide. *IEEE J Sel Top Quantum Electron* 10(1):70–78

Park J (2010) Speedup of dynamic response of organic light-emitting diodes. *J Lightwave Technol* 28(19):2873–2880

Park J, Kawakami Y, Park SH (2007) Numerical analysis of multilayer organic light-emitting diodes. *J Lightwave Technol* 25(9):2828–2836

Park J, Park S, Shin D (2009) Electrical properties of trilayer organic light-emitting diodes with a mixed emitting layer. *J Lightwave Technol* 27(13):2525–2529

Samal GS, Unni KN, Bharat S, Gupta S (2009) Improved efficiency in fluorescent blue organic light emitting diode with a carrier confining structure. *Org Electron* 10(7):1201–1208

Van Veldhoven E, Zhang H, Glasbeek M (2001) Picosecond time-resolved fluorescence depolarization of OLED compounds Alq₃, Gaq₃, and Inq₃. In: *Ultrafast phenomena XII*. Springer, Berlin, pp 482–484

Wakui M, Sameshima H, Hu FR, Hane K (2011) Fabrication of GaN light emitting diode membrane on Si substrate for MEMS applications. *Microsyst Technol* 17(1):109–114

Wen SW, Lee MT, Chen CH (2005) Recent development of blue fluorescent OLED materials and devices. *J Disp Technol* 1(1):90–99

Wu Z, Guo H, Wang J (2007) Highly efficient green top-emitting organic light-emitting devices with metal electrode structure. *Microelectron J* 38(6):686–689

Yang H, Zhao Y, Hou J, Liu S (2006) Organic light-emitting devices with double-block layer. *Microelectron J* 37(11):1271–1275

Yu MH, Tran TH, Hsu YP, Chao PCP, Lee KY, Kao YH (2015) A new prediction model on the luminance of OLEDs subjected to different reverse biases for alleviating degradation in AMOLED displays. *Microsyst Technol* 21(12):2771–2776

Publisher's Note

Springer Nature remains neutral with regard to jurisdictional claims in published maps and institutional affiliations.